2019 12th Asian Control Conference (ASCC)
Kitakyusyu International Conference Center
Japan, June 9-12, 2019

$\mathcal{H}_\infty$ Control of Semi-Active MR Damper Suspensions

Shuyou Yu, Jianjian Zhang, Fang Xu and Hong Chen

***Abstract*— In this paper, control of semi-active suspension with Magneto-rheological (MR) damper is studied to improve the ride comfort of vehicles. The controller is divided into two layers: a constrained $\mathcal{H}_\infty$ output feedback control and an MR damper control. Constrained $\mathcal{H}_\infty$ output feedback control provides the reference of the MR damper control. Ride comfort is chosen as the output performance of $\mathcal{H}_\infty$, and suppressing the hop of the wheels, suspension stroke limitation and saturation limitation of MR damper are time-domain constraints. A feedforward and feedback control law is applied to control the MR damper precisely. Compared with passive suspension system, the proposed scheme can achieve better ride comfort as well as constraint satisfaction.**

***Index Terms*— semi-active suspension, MR damper, $\mathcal{H}_\infty$ output feedback, feedforward and feedback control**

I. INTRODUCTION

Semi-active suspension is a controllable suspension system which is widely used in vehicles. Its vibration attenuation is close to active suspension and its stability is better than passive suspension [1]. Performance requirements for semi-active suspensions include: 1) isolating passengers from vibration and shock arising from road roughness (ride comfort); 2) suppressing the hop of the wheels so as to maintain firm and uninterrupted contact of wheels to road (good handling or good road holding); and 3) keeping suspension strokes within an allowable maximum [2]. These requirements are conflicting, for example, enhancing ride comfort results in larger suspension stroke and smaller damping in the wheel-hop mode. In order to ensure a firm uninterrupted contact of wheels to road, the dynamic tire load should not exceed the static ones [3]. However, occasional and brief excessive wheel-hop on one of the four wheels may be acceptable in some driving situations (e.g., driving on a straight section of the road etc.). Suspensions are placed between the chassis and wheel assembly, hence, structural features of a vehicle impose a strict restriction on the suspension stroke. An excessive suspension bottoming can lead to a considerable deterioration of ride comfort and possible structural damage. These requirements are in fact hard constraints in time-domain and related to safety [4]. The semi-active suspension control problem can then be considered as a disturbance attenuation problem with time-domain hard constraints.

Shuyou Yu, Jianjian Zhang, Fang Xu and Hong Chen are with State Key Laboratory of Automotive Simulation and Control, and with Department of Control Science and Engineering, Jilin University, Changchun 130025, China (e-mail: {shuyou,fangxu,chenh}@jlu.edu.cn, 335887937@qq.com)

The authors gratefully acknowledge support by the National Nature Science Foundation of China (No.6171101085, No.61573165, No.61703176 and No.61520106008).

In order to manage the tradeoff among conflicting performance requirements, many semi-active suspension control approaches are proposed [5]-[7], based on various control techniques such as LQG, adaptive control and nonlinear control. As mentioned in [8] and referenced there in [9]-[11], one of the advantages of these prior designs is that the resulting semi-active suspensions can adapt their gains so as to fully utilize the available suspension stroke and tire deflection. $\mathcal{H}_\infty$ semi-active suspensions are intensively discussed in the context of robustness and disturbance attenuation [12]-[13]. A common point in most approaches is that all requirements, including those associated with hard constraints, are weighted and formulated in a single objective functional ($\mathcal{H}_2$ or $\mathcal{H}_\infty$), which is minimized to find an optimal controller.

Unlike the traditional dampers, MR dampers don't adjust the damping coefficient, but change the coil current to change the damping force [14]. Since the majority of vehicles have the ability to supply the current, it is necessary to produce a controllable variable damper force. Therefore, MR dampers provide an opportunity to solve the problems of ride comfort and stability of semi-active suspension. The complex dynamics of MR dampers reveal the velocity-force characteristics, saturation and hysteresis behavior of their nonlinear relationships [6]. In order to obtain good vibration suppression, it is critical to establish an accurate model of MR damper. Many studies directly regard the semi-active suspension system as the controlled object and the MR damper as the actuator [**?**]-[17]. To implement semi-active suspension control in real time, it is necessary to establish a reversible model of the MR damper. Then the current control signal is obtained by the reversible model, and input to the MR damper to achieve vibration reduction of the entire suspension system.

On the one hand, the damper modeling is highly nonlinear; on the other hand, in order to implement the semi-active control algorithm, it is necessary to establish a reversible model to compensate the nonlinear dynamics [18]. Thus, it is challenging to establish a simple and efficient reversible model which reflects the performance of the MR damper. In addition, in order to achieve high-precision control and improve the robustness and dynamic performance of the control system, closed-loop control of the MR damper is adopted. References [19]-[22] introduce examples of research into suspensions with MR dampers. In majority of these works [18]-[22] the control implementation was not quite suitable for the semi-active and nonlinear hysteretic nature of the MR damper. In the paper [23], the external characteristics of the MR damper were tested. Then the damping force characteris-

tics of the MR damper were expressed by hyperbolic tangent reversible model. Finally, according to the experimental data, the parameters of the model were fitted and verified.

The semi-active suspension can be divided into two parts, a linearized suspension system and a non-linear MR damper system. This paper uses a constrained $\mathcal{H}_\infty$ output feedback control for the linearized suspension. Time-domain output constraints represent, as mentioned previously, the requirements on good road holding and maintaining suspension strokes within bounds. Damping force, generated by MR damper, is bounded because of actuator saturation. Here the $\mathcal{H}_\infty$ performance is used to evaluate ride comfort so that more general road (white noise road) disturbances can be considered. It will be minimized to enhance ride comfort. For the MR damper system, this paper adopts the MR damper model in [24]. The control strategy, using the inverse model as feedforward and actual damping force as feedback, precisely controls the MR damper. Finally, the effectiveness of the control system is verified by a simulation.

II. Problem Setup

Two degree-of-freedom (DOF) one-quarter vehicle model is illustrated in Fig.1, which is simple in construction but contains all the parameters for suspension performance evaluation [25]. In order to facilitate the analysis, the tire is equivalent to a spring, ignoring the tire damping force. In Fig.1, K_s represents the stiffness of the suspension, K_t stands for the tire stiffness, M_2 represents suspended masse, M_1 is the non-suspended mass (tire, damper, spring, etc.). Moreover, Z_2 and Z_1 are the masses displacement, f_d is damping force generated by an MR damper. Z_0 is the vertical displacement of the random road surface in the time domain, which is generated by the filtering white noise method [23]:

$$\dot{Z}_0(t) = -2\pi f Z_0(t) + 2\pi\sqrt{G_0(n_0)\,v}\,\xi(t) \tag{1}$$

where $f = 0.01\text{Hz}$, $G_0(n_0)$ is the road grade, $n_0 = 0.1\text{m}^{-1}$, $\xi(t)$ is unit white noise, v is speed of a vehicle. The dynamic

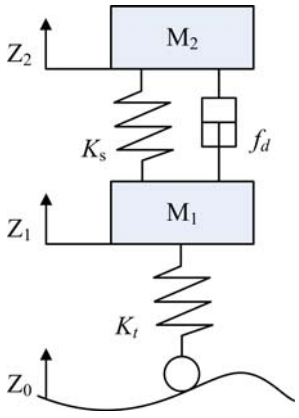

Fig. 1. 2-DOF quarter-car model with a MR damper

of 2 DOF 1/4 vehicle is

$$M_2\ddot{Z}_2 = f_d - K_s(Z_2 - Z_1) \tag{2}$$

$$M_1\ddot{Z}_1 = K_s(Z_2 - Z_1) - K_t(Z_1 - Z_0) - f_d \tag{3}$$

Define

$$\begin{gathered} x_1(t) = Z_2(t) - Z_1(t) \\ x_2(t) = \dot{Z}_2(t) \\ x_3(t) = Z_1(t) - Z_0(t) \\ x_4(t) = \dot{Z}_1(t) \end{gathered}$$

Then the ideal dynamics of the quarter-car model can be described by

$$\begin{aligned} \dot{x}(t) = &\begin{bmatrix} 0 & 1 & 0 & -1 \\ -\frac{K_s}{M_2} & 0 & 0 & 0 \\ 0 & 0 & 0 & 1 \\ \frac{K_s}{M_1} & 0 & -\frac{K_t}{M_1} & 0 \end{bmatrix} x(t) + \\ &\begin{bmatrix} 0 \\ \frac{1}{M_2} \\ 0 \\ -\frac{1}{M_1} \end{bmatrix} f_d(t) + \begin{bmatrix} 0 \\ 0 \\ -1 \\ 0 \end{bmatrix} \dot{Z}_0(t) \end{aligned} \tag{4}$$

The acceleration of the suspension mass is selected as the output of the system, and its expression is

$$y(t) = \begin{bmatrix} -\frac{K_s}{M_2} & 0 & 0 & 0 \end{bmatrix} x(t) + \begin{bmatrix} \frac{1}{M_2} \end{bmatrix} f_d(t) \tag{5}$$

A. MR Damper

The structural principle of a typical shear valve MR damper is shown in Fig.2 [26]. The core components of the MR damper mainly include pistons, coils, magnetic conducting cylinders, compensation cavities and related seals. Since the damping force of the shock absorber is directly related to the magnetic field strength, the effective control of MR damper damping force can be achieved by changing the current in the coil.

The simplified structure of the shear valve MR damper [27] is shown in Fig.3, which is composed of an elastic element, a viscous element and a hysteretic structure.

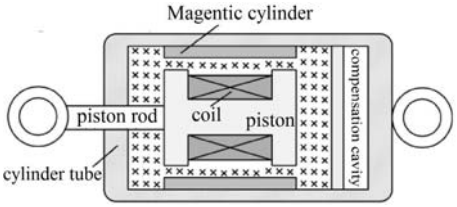

Fig. 2. Structure principle of MR damper

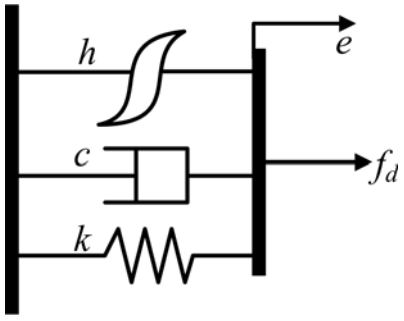

Fig. 3. Simplified structure of MR damper

The dynamic of MR damper is changed from x to e

$$\begin{aligned} f_d &= c\dot{e} + ke + \alpha h + f_0 \\ h &= \tanh\left[\beta\dot{e} + \delta \cdot sign\left(e\right)\right] \end{aligned} \tag{6}$$

where e is elongation or compression displacement of MR damper, c and k are the damping coefficient and the stiffness coefficient, h is the hysteresis variable, f_0 is the compensation value of the damping force, α and β are the scalar factor, δ is coefficient of hysteretic curve.

In order to grasp mapping between the relevant parameters of the MR damper and the current of the excitation coil, MR damper model described in [23] is adopted. Taking data of the dynamics of MR damper under various excitations as samples, four parameters of $c(I)$, $k(I)$, $\alpha(I)$, $f_0(I)$ in the model are identified by the genetic algorithm toolbox. According to the result of parameter identification, the fitting relationship between the parameters and the current of the excitation coil is determined:

$$\begin{aligned} c\left(I\right) &= c_a I + c_b \qquad k\left(I\right) = k_a I + k_b \\ \alpha\left(I\right) &= \alpha_a I + \alpha_b \quad f_0\left(I\right) = f_{0a} I + f_{0b} \end{aligned} \tag{7}$$

where I is the current and the rest are the generation fitting parameters. After establishing the relationship between the parameters and the voltage value, the final expression of the damping force can be obtained as follows

$$\begin{aligned} &f_d\left(e, \dot{e}, I\right) = c\left(I\right)\dot{e} + k\left(I\right)e + f_0\left(I\right) + \alpha\left(I\right)h \\ &h = \tanh\left(\beta\dot{e} + \delta sign\left(e\right)\right) \end{aligned} \tag{8}$$

III. CONTROL STRATEGY

This paper adopts the method of sub-target control. The MR damper is treated as a separate unit in accordance with the nonlinear characteristics of it. We divide the whole semi-active suspension system into two parts: a linear suspension and an MR damper. The sub-target control first formulates the control strategy of the linear suspension part, and the expected control force generated by it is used as the target output of the MR damper. The expected control force is then converted into the input control current of the damper through the damper control so as to realize the tracking of the required control force. The linear suspension section is controlled by $\mathcal{H}_\infty$ output feedback control, and the control of MR damper adopts a feedforward and feedback control strategy. The control principle is shown in Fig. 4.

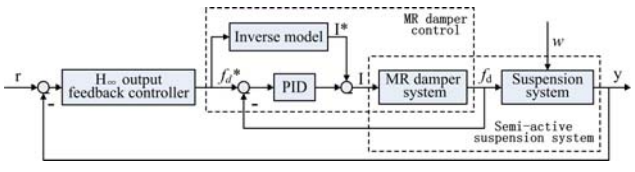

Fig. 4. The control principle of the semi-active suspension

A. Constrained $\mathcal{H}_\infty$ Output Feedback Control

In order to improve the robustness of the suspension system, constrained $\mathcal{H}_\infty$ output feedback control is adopted. Let $f_d = u$ and $w = \dot{Z}_0$, then the ideal dynamics of the quarter-car model can be described by

$$\begin{aligned} \dot{x}\left(t\right) = &\begin{bmatrix} 0 & 1 & 0 & -1 \\ -\frac{K_s}{M_2} & 0 & 0 & 0 \\ 0 & 0 & 0 & 1 \\ \frac{K_s}{M_1} & 0 & -\frac{K_t}{M_1} & 0 \end{bmatrix} x\left(t\right) + \begin{bmatrix} 0 \\ 0 \\ -1 \\ 0 \end{bmatrix} w\left(t\right) \\ &+ \begin{bmatrix} 0 \\ \frac{1}{M_2} \\ 0 \\ -\frac{1}{M_1} \end{bmatrix} u\left(t\right) \end{aligned} \tag{9}$$

$$y(t) = \begin{bmatrix} -\frac{K_s}{M_2} & 0 & 0 & 0 \end{bmatrix} x\left(t\right) + \begin{bmatrix} \frac{1}{M_2} \end{bmatrix} u\left(t\right) \tag{10}$$

The feedback controller is designed to improve the ride comfort of the vehicle, i.e., the semi-active suspension minimizes disturbances on the road when the vehicle is driving on uneven pavement. Therefore, in order to reduce the road surface disturbance, we need to obtain the optimal output damping force of the suspension damper. So this article will take the body acceleration as the performance output:

$$z_1\left(t\right) = \begin{bmatrix} -\frac{K_s}{M_2} & 0 & 0 & 0 \end{bmatrix} x\left(t\right) + \begin{bmatrix} \frac{1}{M_2} \end{bmatrix} u\left(t\right) \tag{11}$$

In order to ensure a firm uninterrupted contact of wheels to road, the dynamic tire load should not exceed the static ones, i.e.

$$K_t\left(Z_1 - Z_0\right) < \left(M_2 + M_1\right)g \tag{12}$$

And, the suspension stroke limitation is in the form of

$$\left(Z_2 - Z_1\right) < \mathrm{S}_{\max} \tag{13}$$

Moreover, considering the output saturation of MR damper, it can only produce limited damping force, that is

$$\left|f_d\right| < \mathrm{U}_{\max} \tag{14}$$

Eqs.(9), (10) and (11) can be treated as time-domain constraints

$$z_2\left(t\right) = \begin{bmatrix} 1 & 0 & 0 & 0 \\ 0 & 0 & 1 & 0 \\ 0 & 0 & 0 & 0 \end{bmatrix} x\left(t\right) + \begin{bmatrix} 0 \\ 0 \\ 1 \end{bmatrix} u\left(t\right) \tag{15}$$

In summary, the goal is to find an $\mathcal{H}_\infty$ output feedback controller, which satisfies the following conditions

1) the closed loop system is stable;
2) $\mathcal{H}_\infty$ norm from the disturbances w to the output z_1 is minimized;
3) constraint z_2 is satisfied.

The constrained $\mathcal{H}_\infty$ output feedback control can be solved by linear matrix inequality (LMI).

Without loss of generality, the system under control can be rewritten as

$$\begin{aligned} \dot{x}\left(t\right) &= Ax\left(t\right) + B_1 w\left(t\right) + B_2 u\left(t\right) \\ z_1\left(t\right) &= C_1 x\left(t\right) + D_{11} w\left(t\right) + D_{12} u\left(t\right) \\ z_2\left(t\right) &= C_2 x\left(t\right) + D_{21} w\left(t\right) + D_{22} u\left(t\right) \\ y\left(t\right) &= C_3 x\left(t\right) + D_{31} w\left(t\right) + D_{32} u\left(t\right) \end{aligned} \tag{16}$$

where $x \in R^n$ is an n-dimensional vector of states, $w \in R^{m_1}$ an m_1-dimensional vector of disturbance inputs, $u \in R^{m_2}$ an m_2-dimensional vector of control inputs, $z_1 \in R^{p_1}$ an p_1-dimensional vector of $\mathcal{H}_\infty$ performance outputs and $z_2 \in R^{p_2}$ an p_2-dimensional vector of constrained outputs, $y \in R^m$ an m-dimensional vector of measurement outputs. From Eq.(4), we can know $D_{21} = 0$ and $D_{31} = 0$, i.e., disturbances have no direct way to affect the constrained outputs and measured output.

Time domain constraints are met if

$$|z_{2i}(t)| \le z_{2i\max}, i = 1, 2, \cdots, p_2, t \ge 0 \tag{17}$$

where $z_{2i,\max}$ is the supremum of constraint.

Assume that

- (A, B_2, C_2) is stabilizable and detectable,
- The disturbance w is unknown, but energy bounded which belongs to the following set:

$$W := \left\{ w \in R^{nw} | \int_0^\infty \|w(\tau)\|_2^2 d\tau \le w_{\max} \right\}$$

Consider the output feedback control law K as

$$\begin{aligned} \dot{\xi}(t) &= A_k \xi(t) + B_k y(t) \\ u(t) &= C_k \xi(t) + D_k y(t) \end{aligned} \tag{18}$$

where $\xi \in R^{nk}$ is the state of controller, A_k, B_k, C_k, D_k is the designed constant matrix with the appropriate dimension.

Denote $x_c = \begin{bmatrix} x & \xi \end{bmatrix}^T$. Substituting the output feedback controller (18) into the system dynamics (16), we can get

$$\begin{aligned} \dot{x}_c(t) &= A_c x_c(t) + B_{c1} w(t) \\ z_1(t) &= C_{c1} x(t) + D_{c1} w(t) \\ z_2(t) &= C_{c2} x(t) + D_{c2} w(t) \end{aligned} \tag{19}$$

where

$$\begin{aligned} A_c &= \begin{bmatrix} A + B_2 D_k C_3 & B_2 C_k \\ B_k C_3 & A_k \end{bmatrix} \\ B_c &= \begin{bmatrix} B_1 + B_2 D_k D_{31} \\ B_k D_{31} \end{bmatrix} \\ C_{c1} &= \begin{bmatrix} C_1 + D_{12} D_k C_{31} \\ D_{12} C_k \end{bmatrix} \\ D_{c1} &= [D_{11} + D_{12} D_k D_{31}] \\ D_{c2} &= [D_{21} + D_{22} D_k D_{31}] \\ C_{c2} &= \begin{bmatrix} C_2 + D_{22} D_k C_3 & D_{22} C_k \end{bmatrix} \end{aligned}$$

Constrained $\mathcal{H}_\infty$ output feedback controller can be reduced to the following semi-definite programming [28]

$$\begin{aligned} &\min_{X>0, Y>0, \hat{A}, \hat{B}, \hat{C}, \hat{D}} \gamma \\ s.t. &\begin{bmatrix} S_0 & S_1 & B_1 + B_2 \hat{D} D_{21} & S_3 \\ * & S_2 & Y B_1 + \hat{B} D_{21} & S_4 \\ * & * & -\gamma I & S_5 \\ * & * & * & -\gamma I \end{bmatrix} < 0 \\ &\begin{bmatrix} \frac{Z}{\lambda} & M_0 & M_1 \\ * & X & I \\ * & * & Y \end{bmatrix} > 0, Z_{ii} \le z_{2i,\max}^2 \end{aligned} \tag{20}$$

where λ is a given parameter, $*$ represents the transpose of a block matrix along a diagonal symmetrical position, I is the unit matrix of the corresponding dimension,

$$\begin{aligned} S_0 &= AX + XA^T + B_2 \hat{C} + \left(B_2 \hat{C} \right)^T \\ S_1 &= \hat{A}^T + A + B_2 \hat{D} C_2 \\ S_2 &= A^T Y + Y A + \hat{B} C_2 + \left(\hat{B} C_2 \right)^T \\ S_3 &= \left(C_1 X + D_{12} \hat{C} \right)^T \\ S_4 &= \left(C_1 + D_{12} \hat{D} C_2 \right)^T \\ S_5 &= \left(D_{11} + D_{12} \hat{D} D_{21} \right)^T \\ M_0 &= C_2 X + D_{22} \hat{C} \\ M_1 &= C_2 + B_{22} \hat{D} C_3 \end{aligned}$$

Suppose that there exists a set of optimal solutions $\left(\gamma^*, X^*, Y^*, \hat{A}^*, \hat{B}^*, \hat{C}^*, \hat{D}^* \right)$, and suppose that there exist a full rank matrix M and N such that $MN^T = I - XY$. Then the parameters of the constrained $\mathcal{H}_\infty$ output feedback controller can be obtained

$$\begin{aligned} \hat{A} :=& N A_k M^T + N B_2 C_3 X + Y B_2 C_k M^T \\ &+ Y(A + B_2 D_k C_3) \\ \hat{B} :=& N B_k + Y B_2 D_k \\ \hat{C} :=& C_k M^T + D_k C_3 X \\ \hat{D} :=& D_k \end{aligned} \tag{21}$$

The output feedback controller K designed according to (21) guarantees that the closed-loop system is internally stable and the $\mathcal{H}_\infty$ norm from $w(t)$ to $z(t)$ is less than γ and time domain hard constraints are satisfied.

B. Control of MR Damper

The mapping from I_d to f_d of MR damper is inverted. In terms of Eq.(7), the inverse model of MR damper is

$$I_d = \frac{f_d - (c_b \dot{x} + k_b x + f_{0b} + \alpha_b \tanh(\beta \dot{x} + \delta sign(x)))}{c_a \dot{x} + k_a x + f_{0a} + \alpha_a \tanh(\beta \dot{x} + \delta sign(x))} \tag{22}$$

which will be used as a feedforward controller in series with the MR damper. Furthermore, in order to track the reference damping force with respect to disturbances or uncertainties, a feedback control is adopted as well. Denote $G_2(s)$ as the MR damper, $G_2^{-1}(s)$ as the inverse model of $G_2(s)$ and $G_1(s)$ as a feedback controller, the control diagram of the MR damper is shown as follows

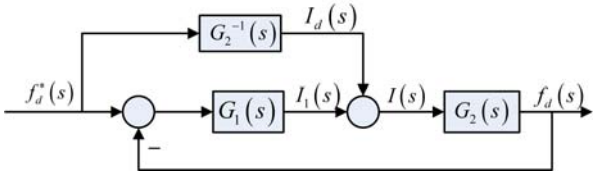

Fig. 5. MR Damper system structure diagram

In terms of

$$\begin{aligned} I_d(s) &= G_2^{-1}(s) f_d^*(s) \\ I(s) &= [f_d^*(s) - f_d(s)] G_1(s) \end{aligned} \tag{23}$$

and

$$\begin{aligned} I(s) &= I_d(s) + I(s) \\ f_d(s) &= I(s) G_2(s) \end{aligned} \tag{24}$$

the closed-loop transfer function of the system is

$$H(s) = \frac{G_2^{-1}(s)G_2(s) + G_1(s)G_2(s)}{1 + G_1(s)G_2(s)} \tag{25}$$

Since, theoretically, $G_2^{-1}(s) = 1/G_2(s)$, $H(s) = 1$, the output can track the ideal input signal

$$\begin{aligned} f_d(s) =& f_d^*(s)H(s) \\ =& f_d^*(s)\frac{G_2^{-1}(s)G_2(s) + G_1(s)G_2(s)}{1 + G_1(s)G_2(s)} \\ =& f_d^*(s) \end{aligned} \tag{26}$$

IV. SIMULATION RESULTS

The simulation is performed on the base of the vehicle speed $60km/h$ and the C-grade pavement, i.e., $G_0(n_0) = 128 \times 10^{-6}$. The random pavement input obtained by SIMULINK is shown in Figure 6.

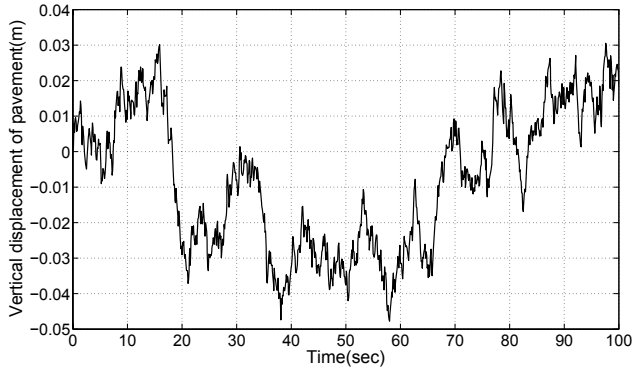

Fig. 6. Random road input

The parameters of the 2-DOF quarter-car model are shown in Tab.1. The polynomial parameters of Eq.(7) and Eq.(8)

TABLE I
PARAMETERS OF 2-DOF QUARTER-CAR MODEL

$M_1(kg)$	$M_2(kg)$	$K_s(N/m)$	$K_t(N/m)$
320	40	18000	200000
$S_{max}(m)$	$U_{max}(N)$	λ	
0.08	800	0.38	

are effectively identified by the least square method, and the results of parameter identification are shown in Tab.2.

The constrained $\mathcal{H}_\infty$ output feedback control law is obtained by solving the convex optimization problem (20)

$$K(s) = \frac{3.43\mathrm{e}^4\mathrm{s}^4 + 2.22\mathrm{e}^6\mathrm{s}^3 + 3.28\mathrm{e}^7\mathrm{s}^2 - 4.63\mathrm{e}^5\mathrm{s} - 1.63\mathrm{e}^7}{\mathrm{s}^4 + 46.58\mathrm{s}^3 + 2030\mathrm{s}^2 + 3.077\mathrm{e}^4\mathrm{s} + 50.86}$$

TABLE II
UNITS FOR MAGNETIC PROPERTIES

Parameter	Values	Parameter	Values
c_a	551.67	c_b	2274.61
k_a	-0.22	k_b	3.57
α_a	168.16	α_b	26.25
f_{0a}	6.62	f_{0b}	182.07
δ	0.74	β	74.65

Under the condition of random white noise road surface, the time domain simulation results of the suspension system are shown in Fig.7, 8 and 9, where semi-active suspension control with closed-loop MR damper (SSC), semi-active suspension control with open-loop MR damper (SSO) and passive suspension (PS) are considered, respectively.

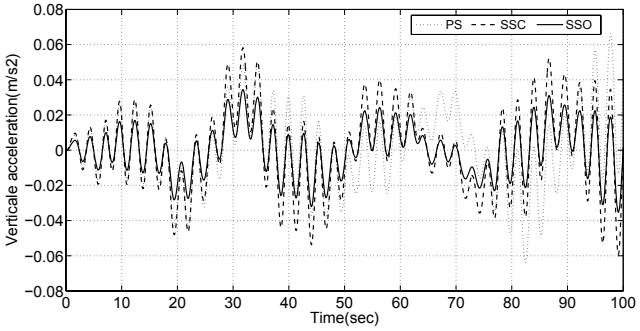

Fig. 7. Vertical acceleration

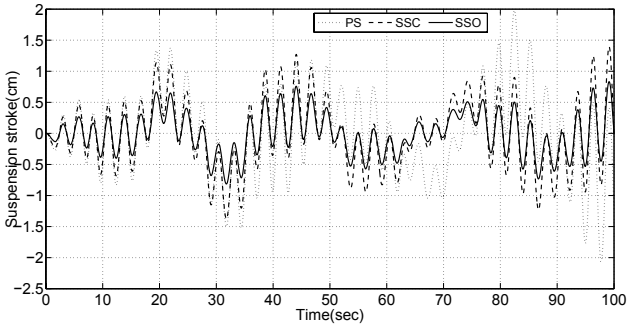

Fig. 8. The suspension stroke

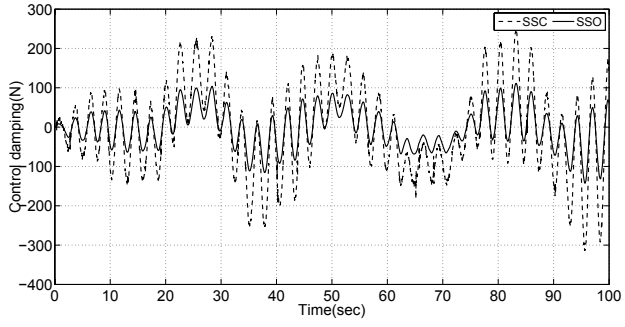

Fig. 9. Semi-active control force

As shown in Fig.7, compared with PS and SSO, the vehicle

vertical acceleration of SSC is greatly reduced and the ride comfort is significantly improved. Furthermore, as the road surface roughness increases and time increases in Fig.6, especially in 60-70 seconds, the ride comfort of SSC is more obvious. In Fig.8, the suspension stroke of SSC is less than the suspension stroke of PS and SSO, of which curve trend is consistent with vehicle vertical acceleration. This is in accordance with the actual situation. While the unevenness of the road surface is within 5cm, the suspension stroke of SSC does not exceed 1cm. Fig.9 shows that the control damping force of SSC and SSO are within the required 800N. Moreover, SSC's control damping force is always smaller than that of B, and the maximum difference is 200 N, which proves that the closed-loop control of the MR damper is effective. In summary, SSC control strategy has a strong ability to attenuate vibration transmitted from road to the human body. At the same time, it can keep the damping force of MR damper within its range and can use the MR damper more accurately.

V. CONCLUSIONS

In this paper, semi-active suspension control problem was formulated as a disturbance attenuation problem with time-domain constraints. In the framework of convex optimization and multi-objective control, a constrained $\mathcal{H}_\infty$ output feedback control approach was presented to manage conflict requirements, i.e., to achieve better ride comfort, while to keep suspension strokes and control inputs within bounds and to ensure firm contact of wheels to road. A feedback control of MR damper determined by its inverse model is adopted to compensate its highly nonlinear properties, and a PID control is to deal with disturbances or model-plant mismatches. Thus, high-precision tracking to the reference given by constrained $\mathcal{H}_\infty$ output feedback control is achieved. Moreover, simulation results confirmed the potential benefit of the proposed constrained $\mathcal{H}_\infty$ semi-active suspension and high-precision tracking of MR damper.

REFERENCES

[1] Yang S Y, Du Y, Qin H M. Control strategy research and experiment verification on active suspension [J]. Modern Manufacturing Engineering, 2017(3):1-6.

[2] Hrovat D. Applications of optimal control to advanced automotive suspension design [J]. ASME Journal of Dynamic Systems Measurement and Control, 1993, 115:328-342.

[3] Gordon T, Marsh C, Milsted M. A comparison of adaptive LQG and nonlinear controllers for vehicle suspension systems [J]. Vehicle System Dynamics, 1991, 20:321-340.

[4] Chen H, Guo K H. Constrained $\mathcal{H}_\infty$ control of active suspensions:An LMI Approach [C]. IEEE Transactions on Control Systems Technology, 2005, 13(3):412-421

[5] Hrovat D. Survey of advanced suspension developments and related optimal control applications [J]. Automation, 1997,33(10):178-1817.

[6] Chen H, Sun P Y, Guo K H. A multi-objective control design for active suspensions with hard constraint [C]. Proceedings of the IEEE American Control Conference, 2003, 5:4371-4376.

[7] Zuo L, Nayfeh S. Structured $\mathcal{H}_2$ optimization of vehicle suspensions based on multi-wheel models [J]. Vehicle System Dynamics, 2003, 40(5):351-371.

[8] Sharkawy A. Fuzzy and adaptive fuzzy control for the automobiles active suspension system [J]. Vehicle System Dynamics, 2005, 43(11):795-806.

[9] Krauze P. Skyhook control of front and rear magnetorheological vehicle suspension [C]. 13th International PhD Workshop OWD 2011, Conference Archives PTETiS, 2011, 29:380-385.

[10] Krauze P. Modelling and identification of magnetorheological vehicle suspension [C]. 17th IEEE International Conference on Methods and Models in Automation and Robotics, 2012:27-30.

[11] Wang H, Xing J T, Price W G, et al. An investigation of an active landing gear system to reduce aircraft vibrations caused by landing impacts and runway excitations[J]. Journal of Sound and Vibration, 2008, 317(1):50-66.

[12] Zapateiro M, Pozo F, Karimi H R, et al. Semiactive Control Methodologies for Suspension Control With Magnetorheological Dampers[J]. IEEE/ASME Transactions on Mechatronics, 2012, 17(2):370-380.

[13] Chen J P, Feng W T, Guo W S. Whole vehicle magnetrorheological fluid damper semi-active suspension variable universe fuzzy control simulation and test [J]. Transactions of the Chinese Society for Agricultural Machinery, 2011, 42(5):7-13.

[14] Alleyne A, Neuhaus P D, Hedrick J K. Application of nonlinear control theory to electronically controlled suspensions [J]. Vehicle System Dynamics, 1993, 22(5):309-320.

[15] Blondel V D, Megretski A. Essentials of robust control [M]. New Jersey: Prentice hall, 1998.

[16] Huang S Y, Chen B, Tu F C. Research on control method for semi-active heavy truck cab mounting system [J]. Journal of Vibration, Measurement and Diagnosis, 2016, 36(1):176-181.

[17] Wen K S, Cuo C, Tian Y T. Optimal control for active engine mount system [J]. Vehicle and Power Technology, 2004, (2):1-4.

[18] Caponetto R, Diamante O, Fargione G, et al. A soft computing approach to fuzzy sky-hook control of semi-active suspension [C]. Transactions on Control Systems Technology, 2003, 11(3):786-798.

[19] Majdoub K E, Ghani D, Giri F Z, et al. Adaptive semi-active suspension of quarter-vehicle with magnetorheological damper[J]. Journal of Dynamic systems, Measurement and Control, 2015, 137(2):1-10

[20] Tuan H D, Ono E, Apkarian P, et al. Nonlinear $\mathcal{H}_\infty$ control for an integrated suspension system via parameterized linear matrix inequality characterizations[C]. IEEE Transactions on Control Systems Technology, 2001, 9(1):175-185.

[21] Sivakumar S, Haran A. Parametric analysis and vibration control of landing gear with PID controller [J]. European Journal of Scientific Research, 2012, 89:441-453.

[22] Tsang H H, Su R K L, Chandler A M. Simplified inverse dynamics models for MR fluid dampers[J]. Engineering Structures, 2006, 28(3):327-341.

[23] Fallah M, Long S, Xie W, et al. Robust model predictive control of shimmy vibration in aircraft landing gears[J]. Journal of Aircraft, 2008, 45(6):1872-1880.

[24] Fan C. Study on Preview Control of Electrorheological Semi-active suspension [D]. Jilin University, 2017.

[25] Batterbee D C, Sims N D. Hardware-in-the-loop simulation of magnetorheological dampers for vehicle suspension systems[J]. Proceedings of the Institution of Mechanical Engineers Part I Journal of Systems and Control Engineering, 2007, 221(2):265C278.

[26] Savaresi S M, Poussot V C, Spelta C,et al. Semi-active suspension control design for vehicles[M]. Elsevier Technology, 2009, 17(1):143-152.

[27] Shi W K, Sun C C, Tian Y T. Optimal control for active engine mount system [J]. Vehicle and Power Technology, 2004, (2):1-4.

[28] Huang S Y, Chen B, Tu F C. Research on control method for semi-active heavy truck cab mounting system [J]. Journal of Vibration, Measurement and Diagnosis, 2016, 36(1):176-181.

[29] Yu S Y, Wang J, Chen H. Output feedback $\mathcal{H}_\infty$ control of constrained linear systems[C]. 2015 10th Asian IEEE Control Conference. Piscataway, N.J, USA, 2015:1-6.